Received: 2 April 2024 | Revised: 21 May 2024 | Accepted: 24 May 2024

DOI: 10.1002/pol.20240262

RESEARCH ARTICLE

JOURNAL OF POLYMER SCIENCE WILEY

Polysaccharide-based H_2S donors: Thiol-ene functionalization of amylopectin with H_2S-releasing *N*-thiocarboxyanhydrides

Abigail F. Chinn[1,2] | **Noah R. Williams**[1,2] | **Kevin M. Miller**[3] | **John B. Matson**[1,2]

[1]Department of Chemistry, Virginia Tech Center for Drug Discovery, Virginia Tech, Blacksburg, Virginia, USA

[2]Macromolecules Innovation Institute, Virginia Tech, Blacksburg, Virginia, USA

[3]Department of Chemistry, Murray State University, Murray, Kentucky, USA

Correspondence
John B. Matson, Department of Chemistry, Virginia Tech Center for Drug Discovery, Virginia Tech, Blacksburg, VA 24061, USA.
Email: jbmatson@vt.edu

Funding information
Division of Materials Research, Grant/Award Number: DMR-1933525

Abstract

Polymeric donors of gasotransmitters, gaseous signaling molecules such as hydrogen sulfide, nitric oxide, and carbon monoxide, hold potential for localized and extended delivery of these reactive gases. Examples of gasotransmitter donors based on polysaccharides are limited despite the availability and generally low toxicity of this broad class of polymers. In this work, we sought to create a polysaccharide H_2S donor by covalently attaching *N*-thiocarboxyanhydrides (NTAs) to amylopectin, the major component of starch. To accomplish this, we added an allyl group to an NTA, which can spontaneously hydrolyze to release carbonyl sulfide and ultimately H_2S via the ubiquitous enzyme carbonic anhydrase, and then coupled it to thiol-functionalized amylopectin of three different molecular weights (MWs) through thiol-ene "click" photochemistry. We also varied the degree of substitution (DS) of the NTA along the amylopectin backbone. H_2S release studies on the six samples, termed amyl-NTAs, with variable MWs (three) and DS values (two), revealed that lower MW and higher DS led to faster release. Finally, dynamic light scattering experiments suggested that aggregation increased with MW, which may also have affected H_2S release rates. Collectively, these studies present a new synthetic method to produce polysaccharide H_2S donors for applications in the biomedical field.

KEYWORDS

biomacromolecules, carbonic anhydrase, COS, release rates

1 | INTRODUCTION

Polymer drug delivery vehicles are used clinically to improve aqueous solubility,[1,2] target release to specific organs and systems,[3,4] and tune delivery rates,[5,6] among other roles.[7,8] However, bioaccumulation, immune system responses, and lack of degradability are concerns with many polymers currently used in drug delivery (e.g., poly (ethylene glycol), PEG).[9] Polysaccharides are poised to help solve these problems due to features including aqueous solubility, biodegradability, minimal toxicity, drug stabilization, and widespread availability typically at low cost.[10–15] In fact, several types of polysaccharide drug delivery vehicles are under investigation, including

nanoparticles,[16,17] hydrogels,[18,19] and polysaccharide-drug conjugates.[20,21] Polysaccharide-based drug delivery vehicles are poised to continue to improve drug delivery efficacy and safety.

One potential drug in need of effective delivery methods is H_2S, an endogenous signaling gas with many physiological roles.[22,23] H_2S, which was the last of the three widely accepted gasotransmitters to be discovered in 1996,[24] affects nearly all organs and systems and is a global regulator of gene expression.[25] H_2S deficiency can lead to heart failure, hypertension, preeclampsia, liver disease, and Alzheimer's disease, among many other complications and disorders.[25,26] Gut microbiome health and behavior are also affected by H_2S levels.[27,28] Therefore, small molecules, polymers, and materials that release H_2S, collectively termed H_2S donors, find use both as tools to study the endogenous roles of H_2S and also have potential therapeutic value as pharmaceuticals to help combat complications caused by H_2S deficiencies.[29–32]

While the majority of H_2S donors reported thus far have been small molecules, polymeric donors have gained interest due to their ability to influence drug release kinetics, target delivery to specific organs and subcellular organelles, localize release via hydrogels or implantable materials, and co-deliver H_2S with other compounds (Figure 1A).[31,33–37] For example, Li and coworkers synthesized a light-triggered, water-soluble polymeric H_2S donor.[38] The polymer backbone was synthesized via reversible addition−fragmentation chain transfer (RAFT) polymerization and further modified to attach nitrobenzenemethanethiol units, which degraded under UV irradiation to afford H_2S. Other work includes attaching small molecule H_2S donors, such as trisulfides,[39] dithiol thiones,[40] and *S*-aroylthiooximes,[41] to polymer backbones. H_2S can also be generated from carbonyl sulfide (COS),[30] which the ubiquitous enzyme carbonic anhydrase (CA) converts into H_2S.[42] Our group and others have developed several types of COS donors,[43–47] and these have been translated to polymers.[47,48] For example, a water-soluble poly(acryloyl morpholine) with an *N*-thiocarboxyanhydride (NTA) on the chain end afforded a water-soluble polymeric H_2S donor.[47]

While polymeric H_2S donors have gained popularity, the only polysaccharide H_2S donor that we are aware of is a hyaluronic acid derivative modified with ADT, a dithiolethione H_2S donor (Figure 1A).[49] This water-soluble H_2S donor suppressed the growth of human breast cancer cells. The mechanism of H_2S release from diolthiol-thiones has been the subject of some debate, but recent evidence suggests that it releases H_2S in response to oxidants such as hydrogen peroxide,[50] which are often overproduced in the tumor microenvironment. Inspired by this work, we set out to conduct a systematic study on a set of polysaccharide-based H_2S donors with appended NTAs, which avoid the need for H_2O_2 because they are spontaneous COS/H_2S donors. We chose amylopectin as a simple polysaccharide backbone (Figure 1B). Amylopectin is the partially water-soluble, branched portion of starch and is its main component; it is naturally found with a molecular weight exceeding 1,000,000 g/mol and repeating α-D-(1 → 4) glycosidic linkages with branching on the C6 hydroxyl unit. It is used in the biomedical industry, mostly for drug delivery applications,[51–53] and the hydroxyl units on amylopectin provide a functional group handle for modification.

We envisioned that an amylopectin-based H_2S donor would provide a water-soluble polymeric donor that possesses low toxicity, biological degradability, and prolonged release rates. Specifically, we aimed to functionalize amylopectin with NTAs and study how the degree of substitution (DS) and molecular weight (MW) influence the

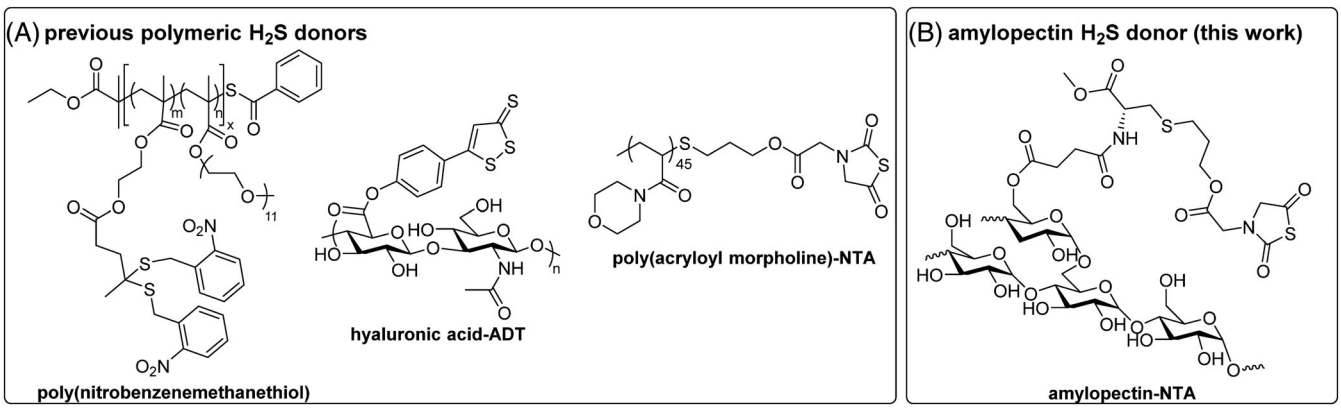

FIGURE 1 (A) Previous polymeric H_2S donors synthesized including one polysaccharide (hyaluronic acid) H_2S donor.[38,47,49] (B) Polysaccharide (amylopectin) H_2S donor demonstrated in this work. Substitution only at the 6 position is shown for sake of clarity but is not meant to imply regioselectivity.

release rates of H_2S. Based on trends observed in other polymeric drug-delivery vehicles in the literature, we hypothesized that H_2S release rates would increase with decreasing amylopectin molecular weight and with decreasing levels of NTA substitution.

2 | RESULTS AND DISCUSSION

Natural amylopectin has a very high MW (>1,000,000 g/mol),[54] so main-chain degradation would be needed to achieve lower MWs. This was critical both to improve solubility and to create a series of MWs to evaluate how this parameter affected H_2S release. O'Neill and coworkers have shown that aqueous HCl degrades amylopectin via random chain scission such that MW decreases with time.[55,56] We degraded amylopectin in 1 M HCl at 50 °C, removing aliquots at various time points, and the acid-degraded amylopectin was then precipitated into methanol and recovered by filtration. Attempts to characterize these polymers using size-exclusion chromatography with multi-angle light scattering (SEC-MALS) in $H_2O/NaNO_3$ were unsuccessful due to limited solubility.

In order to improve their solubility for SEC-MALS, we functionalized each sample with succinic anhydride to a target DS of 0.25 to afford amyl-COOH derivatives. This procedure led to improved water solubility that was sufficient for SEC-MALS analysis in $H_2O/NaNO_3$ (Figure S18; Tables 1 and S1). SEC traces were multimodal for samples removed at earlier time points with high molar masses and molar mass dispersity ($Đ$) values near 4.5. Traces became unimodal as the acid degradation procedure reduced the MW; for example, the sample removed at 20 h reached 65,400 g/mol and $Đ = 4.2$, and the sample removed after 7 days reached 12,200 g/mol and $Đ = 1.7$. Plotting number-average molar mass (M_n) determined by SEC-MALS versus acid degradation time revealed an exponential decrease over time (Figures 2, S18, and S19). The degradation behavior is seen more easily using a linear fit to a log–log plot of M_n versus acid degradation time (Figures 2 inset and S19).[54] We chose to move forward with samples degraded for 10 min ($M_n = 154$ kg/mol, high MW), 20 h ($M_n = 65.4$ kg/mol, med MW), and 7 days ($M_n = 12.2$ kg/mol, low MW), which afforded a range of MWs.

We next set out to attach a small molecule H_2S donor, an NTA, to the acid-degraded amylopectin samples. We previously developed a variety of methods to attach an NTA to another compound or polymer, including copper-catalyzed azide-alkyne cycloaddition reactions, olefin metathesis, and the thiol-ene reaction.[47] These reactions all rely on modification of NTAs with a variety of functional groups—including allyl, alkynyl, azido, and norbornenyl groups—which can then be used for further derivatization. Here, we sought to attach an NTA to amylopectin through thiol-ene "click" photochemistry due to its lack of metal catalysts, application in the biomedical field, and typically high conversion.[58] Therefore, we aimed to use our previously reported allyl-NTA and add it to thiol-functionalized amylopectin.

Previous efforts to functionalize amylopectin (or unfractionated starch) with thiol groups include reacting starch with cysteine under acidic conditions,[59] forming starch-xanthate using carbon disulfide and then pyrolyzing to afford starch-thiol,[60] and attaching of

TABLE 1 Molecular weights (MW) data of amyl-COOH derivatives.

Label	Acid degradation time	M_n (kg/mol)$_{SEC\text{-}MALS}$[a]	$Đ$[a]
High MW	10 min	154	4.4
Med MW	20 h	65.4	4.2
Low MW	7 days	12.2	1.7

[a]M_n and dispersity ($Đ$) determined by size-exclusion chromatography with multi-angle light scattering (SEC-MALS) in $H_2O/NaNO_3$ at 40 °C, 1 mL/min. All samples used $dn/dc = 0.156$ mL/g based on a literature value.[57] SEC traces are in Figure S18.

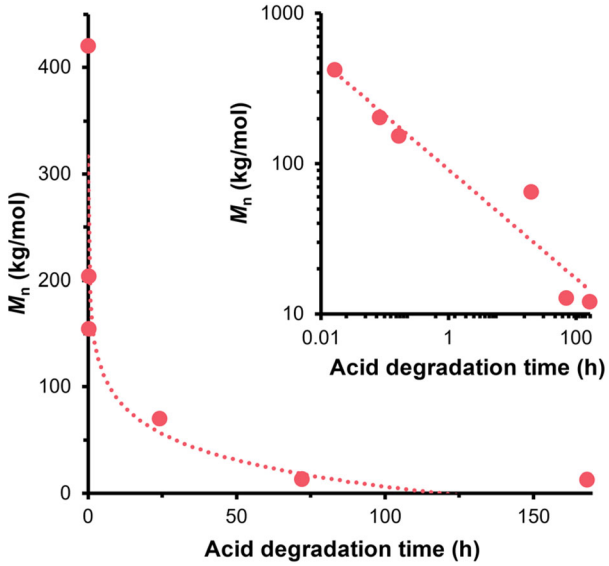

FIGURE 2 Plot of measured M_n values of amyl-COOH derivatives versus acid degradation time. M_n values were measured using SEC-MALS (eluent $H_2O/NaNO_3$ and $dn/dc = 0.156$ mL/g based on a reported value[57]). The inset shows the log–log plot of the same data. Log–log plots for both M_n and M_w as a function of acid degradation time and corresponding fit-line equations are in Figure S19. SEC-MALS numerical data is tabulated in Table S1.

cysteine to starch functionalized with a carboxylic acid,[61] as well as other methods.[62,63] We originally evaluated coupling the carboxylic acid functional group on *N*-acetyl cysteine directly to the alcohols on amylopectin utilizing *N*-(3-dimethylaminopropyl)-*N*-ethylcarbodiimide (EDC). ^{1}H NMR spectroscopy showed limited conversion (Figure S23), and water solubility was low. Given the increased water solubility of the amyl-COOH derivatives utilized for SEC analysis, we reasoned that the water solubility of thiol-functionalized amylopectin derivatives would improve if we started from these amyl-COOH samples. In brief, we envisioned that EDC could promote coupling of a cysteine methyl ester derivative, H-Cys-OMe, with carboxylic acid functional groups on amyl-COOH samples. In fact, Wang and coworkers applied a similar two-step succinylation-coupling method to add cysteine to starch.[61] The authors created hydrogels from these materials by oxidizing the thiols to form disulfide bonds, but we anticipated that this synthetic approach could work well to functionalize amylopectin with allyl-NTA.

First, we synthesized amyl-COOH derivatives of each of the three amylopectin samples of different MWs using succinic anhydride as discussed above (Scheme 1). The DS could be easily adjusted in this succinylation step by changing the equivalents of succinic anhydride with respect to alcohols. Formation of amyl-COOH was confirmed by ^{1}H NMR spectroscopy in D_2O, and DS was calculated based on the integral ratios of relevant peaks, specifically the anomeric proton and the methylene protons alpha to the amylopectin ester (Figures S3, S12–S17). Two different DS values were used in this study: DS 'high', which had a theoretical DS of 0.25, and DS 'low', which had a theoretical DS of 0.125. Actual values were close to these targets. As three different MWs were used for each, a total of 6 amyl-COOH samples were prepared (DS(high)-MW(high), DS(high)-MW(med), DS(high)-MW(low), DS(low)-MW(high), DS(low)-MW (med), DS(low)-MW(low)). After succinylation, each of these six amyl-COOH samples was purified via dialysis against water (MWCO 6–8 kg/mol) and then recovered by lyophilization.

Next, we coupled H-Cys-OMe to each of the six amyl-COOH samples using EDC to afford six amylopectin-thiol samples (amyl-SH). EDC couplings were performed in phosphate buffer (0.01 M, pH = 6), and the six amyl-SH products were similarly purified using dialysis against water (MWCO 6–8 kg/mol) and isolated as white powders after lyophilization. Successful conversion to the desired products was confirmed by ^{1}H NMR spectroscopy in D_2O (Figures S4, S12–S17). Reaction conversion was estimated based on the integral ratios of the anomeric proton and the methyl protons on the methyl ester of cysteine. Conversions ranged from 67% to 96% based on these estimations, suggesting that DS values remained fairly close to the original target values of 0.25 (high) and 0.125 (low).

With the six amyl-SH samples in hand, we next set out to find ideal conditions for the thiol-ene reaction. To test the conditions, we first evaluated conditions using small molecule model compounds, specifically *N*-acetyl cysteine (Ac-Cys-OH) and allyl-NTA, using diphenyl(2,-4,6-trimethylbenzoyl)phosphine oxide (TPO) as a photoinitiator under long-wave UV light (Scheme 2).

We began with a series of solvent screenings. Amyl-SH is water soluble, whereas allyl-NTA and TPO are organic soluble; therefore, we needed to find a solvent system that solubilized both. The model reaction in water

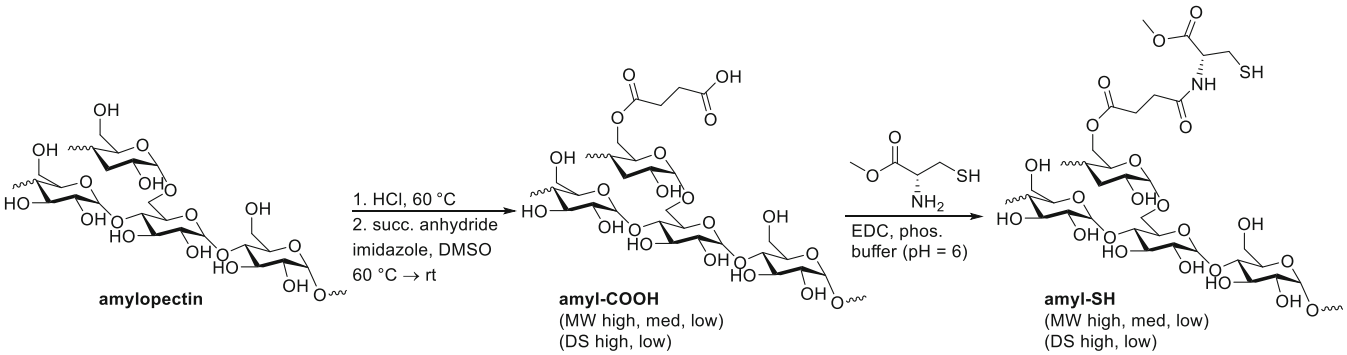

SCHEME 1 Synthesis of six amyl-SH samples. First, amylopectin was subjected to acidolysis to make three samples of amyl-COOH with three different molecular weights (MWs) (high, medium, and low). Next, each amylopectin sample was succinylated via ring-opening of succinic anhydride at two different degree of substitution (DS) (high and low) values to afford six total amyl-COOH samples. Finally, H-Cys-OMe was added in an *N*-(3-dimethylaminopropyl)-*N*-ethylcarbodiimide (EDC) coupling reaction to each of the six amyl-COOH samples to afford six amyl-SH samples with varying molecular weight (high, medium, low) and DS (high, low). Substitution only at the 6 position is shown for sake of clarity but is not meant to imply regioselectivity.

afforded no conversion (Table 2, Figure S9), presumably due to low solubility of allyl-NTA and the TPO photoinitiator. Hexafluoroisopropanol (HFIP) and acetone both afforded low conversions, 9% and 15%, respectively. Next, we investigated systems involving both water and water-miscible organic solvents. Acetone was chosen due to the increased stability of allyl-NTA in acetone compared to other water-miscible solvents, including alcohols and dimethyl sulfoxide. A 75:25 acetone:H_2O solvent system afforded the target product in 56% conversion, while shifting to a 50:50 ratio of these two solvents showed 82% conversion. Mixtures of acetone and H_2O with less than 50% acetone were not evaluated due to insolubility of TPO and allyl-NTA. Water and HFIP solvent systems were tested with 0.1 equiv of TPO while the other solvents systems were tested with 0.05 equiv TPO. The final product, Cys-NTA, was confirmed using ^{1}H and ^{13}C NMR spectroscopy as well as mass spectrometry (Figures S5–S8).

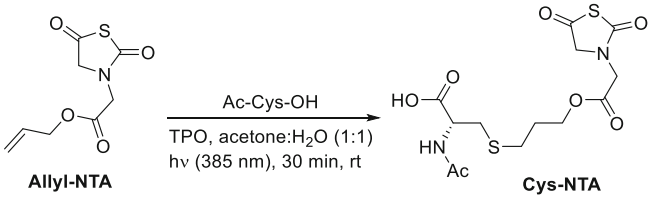

SCHEME 2 Model compound studies in the synthesis of Cys-NTA using Ac-Cys-OH and allyl-NTA via thiol-ene "click" photochemistry.

TABLE 2 Conversion data for various thiol-ene conditions.

Solvent	Molar Equiv TPO	% Conversion[a]
Water	0.1	0
HFIP	0.1	9
Acetone	0.05	15
75:25 acetone:H_2O	0.05	56
50:50 acetone:H_2O	0.05	82
50:50 acteone:H_2O	0.1	90
50:50 acteone:H_2O	0.2	>99

[a]Conversion measured using ^{1}H NMR spectroscopy (Figure S9).

After arriving at a suitable solvent system, we systematically varied the amount of TPO in the small molecule thiol-ene reaction. Usually thiol-ene reactions require small amounts of photoinitiator, often in the range of 0.01–0.05 equiv with respect to thiol and alkene reactants. However, we found that 0.2 equiv was required for quantitative conversion (Table 2; Figure S9), with 0.05 and 0.1 equiv of TPO leading to lower conversions, 82% and 90%, respectively. This high loading requirement may be due to allyl-NTA retarding radical production, although it was not clear based on ^{1}H NMR experiments why so much TPO was needed to reach full conversion.

Using the synthetic method that we optimized in the small molecule analogue reactions, we then set out to convert all 6 amyl-SH samples into amyl-NTAs (Scheme 3). Each of the amyl-SH samples [DS(high)-MW(high), DS(high)-MW(med), DS(high)-MW(low), DS(low)-MW(high), DS(low)-MW(med), DS(low)-MW (low)] were functionalized with a COS/H_2S donating NTA. Amyl-SH and allyl-NTA were coupled using thiol-ene "click" photochemistry with TPO photoinitiator (0.3 equiv with respect to alkene) in a water/acetone mixture as optimized in the small molecule studies described above. Products were purified using dialysis against

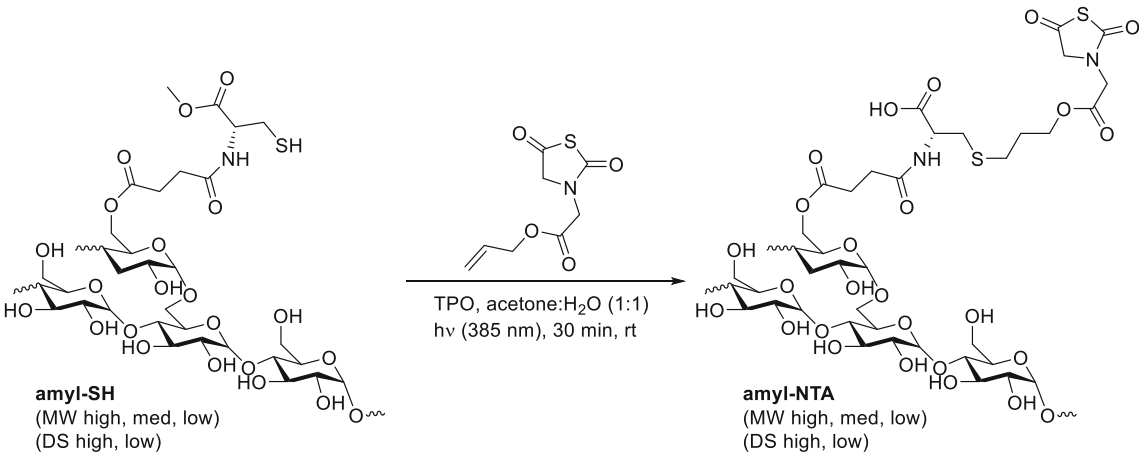

SCHEME 3 Synthesis of six amyl-NTA samples (with three different MW values and two DS values). Each amyl-SH sample was coupled with allyl-NTA via a thiol-ene "click" reaction with diphenyl(2,4,6-trimethylbenzoyl)phosphine oxide (TPO) photoinitiator. Substitution only at the 6 position is shown for sake of clarity but is not meant to imply regioselectivity.

acetone (MWCO 6–8 kg/mol), leading the products to precipitate into the dialysis tubing. The recovered solids were solubilized in water and then lyophilized to afford white powders. Product identities were confirmed using ^{1}H NMR spectroscopy in D_2O (Figures S10, S12–S17).

The derivatization of amylopectin to afford amyl-COOH, amyl-SH, and finally amyl-NTA was followed using Fourier transform infrared spectroscopy (Figure 3). Amylopectin has a weak and broad signal in the 1650–1700 cm^{-1} range due to O-H bends (gray trace).[64,65] Addition of succinic anhydride revealed two overlapping peaks near 1725 cm^{-1} (blue trace) consistent with the addition of an ester and a carboxylic acid. Following EDC coupling with cysteine methyl ester, a stretch corresponding to the newly added cysteine amide appeared at 1646 cm^{-1} (purple trace). A trace of small molecule allyl-NTA (light red) had two carbonyl peaks, one near 1725 cm^{-1} and one at 1682 cm^{-1}. After the thiol-ene reaction with allyl-NTA, the resulting amyl-NTA showed peaks at 1646, 1682, and 1725 cm^{-1}, consistent with the expected carbonyl stretches. Overall, the IR data corroborated our conclusions from the NMR experiments.

We estimated total NTA loading on each of the six samples using elemental analysis, specifically following sulfur content, due to the potential for error when integrating small peaks in the NMR spectra (Tables 3, S2; Figures S20, S21). Results indicated that the reactions were successful, but that either the reactions did not reach full conversion, or that the NTAs hydrolyzed during the dialysis step. For example, for the three samples with NTA DS 'high' (target DS = 0.25), the NTA DS values estimated by elemental analysis were 0.075, 0.103, and 0.050 for the high, med, and low MW samples, respectively (Table 3). For the samples with NTA DS 'low' values (target DS = 0.125), the estimated DS values were 0.037, 0.067, and 0.045 for the high, med, and low MW samples, respectively. Even though DS values were below target marks, each respective MW held both a DS 'high' and DS 'low' sample; the overall range of DS values still allowed us to compare H_2S release rates based upon DS. DS values estimated by ^{1}H NMR spectroscopy were comparable to values determined using elemental analysis (Figures S12–S17).

We next monitored H_2S release from each of the six amyl-NTA derivatives. To measure the H_2S release rate, we used the methylene blue assay, a common method for following H_2S release kinetics.[66-69] In brief, the methylene blue assay involves trapping H_2S as insoluble ZnS, followed by conversion of the trapped sulfide into methylene blue by addition of acidic solutions of *N*,*N*-dimethyl-*p*-phenylene diamine and $FeCl_3$.[70] In the case of COS donors, CA must be included in the assay to convert COS into H_2S. Methylene blue concentration is easily quantified using a plate reader and following the absorbance peak at 750 nm.

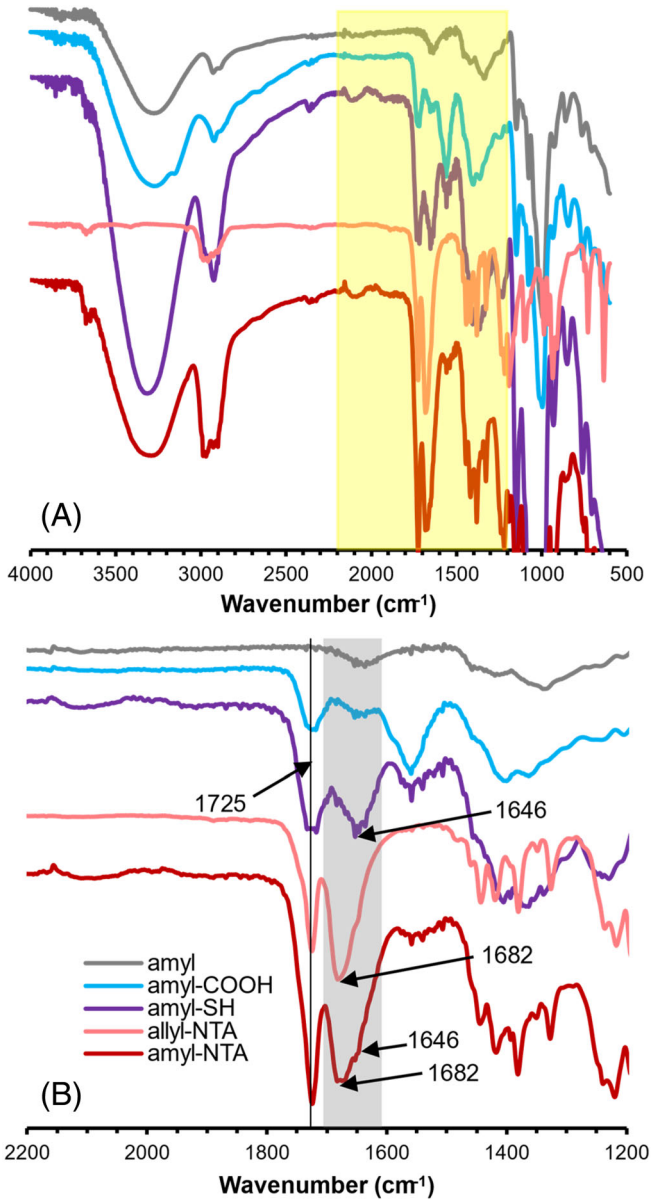

FIGURE 3 Representative Fourier transform infrared spectra of amyl derivatives [amylopectin as received (gray) amyl-COOH (light blue), amyl-SH (purple), and amyl-*N*-thiocarboxyanhydride (NTA) (dark red)] as well as allyl-NTA (light red). (A) Full spectrum, (B) zoomed-in area highlighting the carbonyl peaks. The black line highlights the carbonyl stretches at 1725 cm^{-1}, where carboxylic acids, esters, and one of the NTA carbonyl groups overlap. The region screened in gray indicates variable peaks including the amide stretch at 1646 cm^{-1} and the other NTA carbonyl stretch at 1682 cm^{-1}.

We measured the release rate of all six amyl-NTA polymers as well as a water-soluble small molecule analogue (sarcosine-NTA, Sar-NTA, Figure S11) using the methylene blue assay with added CA (Figures 4, S24,

TABLE 3 Total *N*-thiocarboxyanhydrides (NTA) degree of substitution (DS) on amyl-NTA derivatives.

Theo DS	MW	NTA DS
High	High MW	0.075
High	Med MW	0.103
High	Low MW	0.050
Low	hi|Gh MW	0.037
Low	Med MW	0.067
Low	Low MW	0.045

Note: NTA DS values on amyl-NTA derivatives were estimated by sulfur atom elemental analysis. The elemental analyzer was calibrated against a cysteine standard. Elemental analysis can be found in Figure S20.

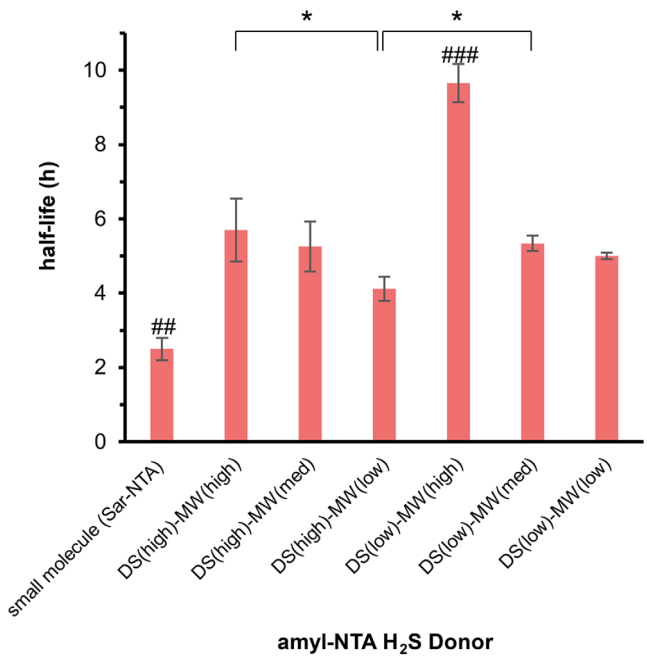

FIGURE 4 H_2S release rate half-lives across different amylopectin molecular weights (MWs) and *N*-thiocarboxyanhydride (NTA) degree of substitution (DS) values. MW values are 154, 65.4, and 12.2 kg/mol for high, med, and low, respectively (Figures S24–S37). The error bars represent standard deviation. ### indicates $p < 0.0001$ and ## indicates $p < 0.01$ for a comparison versus all other groups, using Tukey–Kramer HSD. * indicates $p < 0.05$ among indicated groups. Statistical data can be found in Table S4.

S25). We chose Sar-NTA, which is derived from sarcosine, because previous work from our group demonstrated that the H_2S release rate of small molecule *N*-substituted NTAs has little dependence on *N*-atom substitution, but polymeric NTAs release H_2S more slowly than small molecules.[47] We considered using allyl-NTA as the small molecule H_2S donor, but it is not readily soluble in phosphate buffer. Sar-NTA, however, is soluble in phosphate buffer, which allowed for standardization of methods. Results showed that Sar-NTA had a release half-life of 2.5 ± 0.3 h (Figure 4 and S24, S25).

The H_2S release data using the methylene blue assay for each of the six compounds revealed several interesting trends and insights (Figure 4). First, all of the polymers released H_2S slower than the small molecule Sar-NTA, with half-lives ranging from 4 to 10 h. These relatively long release half-lives by the polymeric H_2S donors may be useful, for example, in gastrointestinal applications where longer release times allow for longer therapeutic time and fewer issues with patient compliance.[71] It can take upwards of 8 h for substances to move through the stomach and small intestine.[72] The polysaccharide H_2S donor increases the half-life from 3 h to around 6 h, doubling the potential therapeutic time and increasing chances of H_2S reaching the small intestine instead of only the stomach.

Second, we originally hypothesized that lower NTA DS would lead to a decrease in release half-life (increase in release rate). Upon comparing the release half-lives for each of the MWs with the varying DS levels, release half-life decreased as DS increased in two of the pairs. For the two high MW samples, the half-life decreased from 9.7 ± 0.5 to 5.7 ± 0.8 h with increasing DS, and for the low MW samples, the half-life decreased from 5.0 ± 0.1 to 4.1 ± 0.3 h with increasing DS. These differences refute our hypothesis with respect to DS. This may be due to residual (unreacted) Cys-OMe thiols increasing H_2S solubility in the high DS samples, increasing COS/H_2S release rates. The similar release rates among the two medium MW samples may be due to their overall higher DS values than the other samples. The third trend we noticed was that the release half-life depended on amylopectin MW. Here we hypothesized that release half-life would decrease (rate would increase) with decreasing MW, and this was the case for both the DS 'high' and the DS 'low' series across the three different MWs. Statistical analyses are described in the SI (Table S4).

Finally, we collected dynamic light scattering (DLS) data on each of the six amyl-NTA samples (Figures 5 and S22; Table S3). Particles on the order of 50–500 nm were observed in all samples, indicating aggregation. In general, particle size as measured by intensity average and *z*-average tended to increase with increasing amylopectin MW. In contrast, aggregate size measured by DLS did not depend on DS. As DLS results can vary widely for polydisperse samples such as these, for example depending on sample preparation methods and fitting routines, we hesitate to draw strong conclusions. However, it is clear that DLS results followed the general trend that as MW

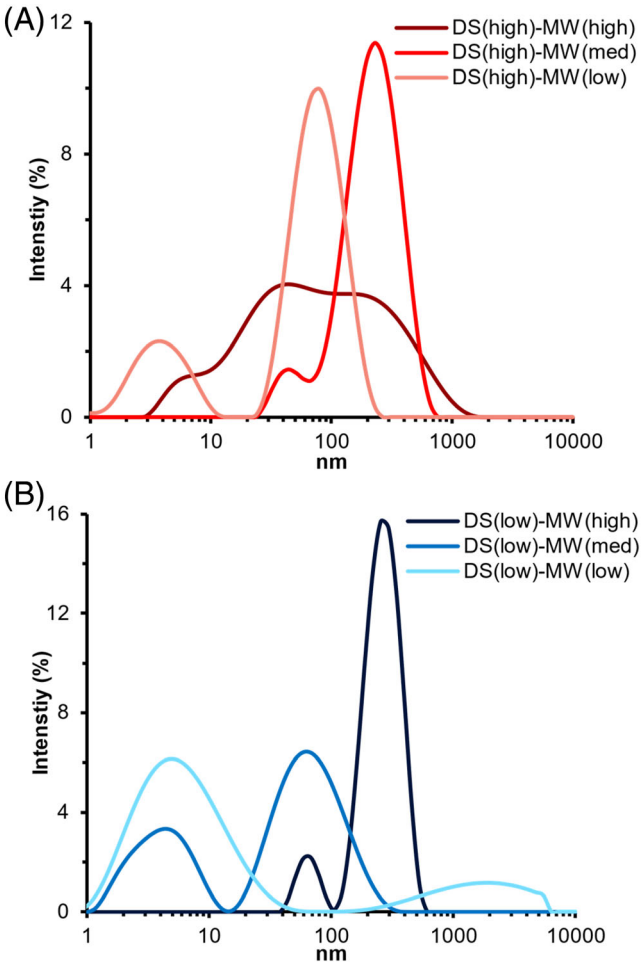

FIGURE 5 Dynamic light scattering (DLS) intensity average traces for all 6 amyl-SH samples [(DS(high)-MW(high), DS(high)-MW(med), DS(high)-MW(low), DS(low)-MW(high), DS(low)-MW (med), DS(low)-MW(low)] at 1 mg/mL in H_2O. DLS data can be found in Figure S22 and Table S3.

increases, aggregate size increases, and the release half-life increases.

3 | CONCLUSIONS

In summary, we synthesized six different polysaccharide H_2S donors via acidolysis of amylopectin followed by multiple side-chain modification steps. We hypothesized that varying both the amylopectin MW and the DS of the NTA COS/H_2S donor along the amylopectin backbone would affect the release rate of COS/H_2S. Ultimately, higher DS and lower MW accelerated H_2S release (i.e., half-life decreased). These findings represent the first systematic study of polysaccharide-based H_2S donors, and release trends are generally in agreement with other polymeric drug delivery vehicles. DLS data suggested that part of the effect might be due to aggregation in aqueous solution. Ultimately, the relatively long (hours) and moderately tunable release rate afforded from this polysaccharide-NTA system, which is water-soluble, may find use in delivery of H_2S to the gut. Furthermore, these results pave the way for rational development of polysaccharide-based H_2S donors for use in many potential biomedical applications.

ACKNOWLEDGMENTS

This work was supported by GlycoMIP, a National Science Foundation (NSF) Materials Innovation Platform funded through Cooperative Agreement DMR-1933525. This work used shared facilities at the Nanoscale Characterization and Fabrication Laboratory, which is funded and managed by Virginia Tech's Institute for Critical Technology and Applied Science. Additional support for the DLS studies was provided by the Virginia Tech National Center for Earth and Environmental Nanotechnology Infrastructure (NanoEarth), a member of the National Nanotechnology Coordinated Infrastructure (NNCI), supported by NSF (ECCS 1542100 and ECCS 2025151). We thank Dr. Brady Hall for performing SEC-MALS analysis, and Dr. Kevin Edgar, Dr. Zhao Li, Sarah Swilley, and Anna Steele for helpful suggestions. We thank Ishani Sarkar for help with statistical analysis.

CONFLICT OF INTEREST STATEMENT

The authors declare no conflict of interest.

ORCID

Abigail F. Chinn https://orcid.org/0000-0003-4829-2914
Kevin M. Miller https://orcid.org/0000-0001-5314-7477
John B. Matson https://orcid.org/0000-0001-7984-5396

REFERENCES

[1] W. Xu, P. Ling, T. Zhang, *J. Drug Delivery* **2013**, *2013*, 340315.
[2] H. Bader, H. Ringsdorf, B. Schmidt, *Angew. Makromol. Chem.* **1984**, *123*, 457.
[3] M. Z. Khan, H. P. Stedul, N. Kurjaković, *Drug Dev. Ind. Pharm.* **2000**, *26*, 549.
[4] P. Abasian, S. Shakibi, M. S. Maniati, S. Nouri Khorasani, S. Khalili, *Polym. Adv. Technol.* **2021**, *32*, 931.
[5] S. A. Bravo, M. C. Lamas, C. J. Salamón, *J. Pharm. Pharm. Sci.* **2002**, *5*, 213.
[6] A. Geraili, M. Xing, K. Mequanint, *View* **2021**, *2*, 20200126.
[7] H. Liu, L. S. Taylor, K. J. Edgar, *Polymer* **2015**, *77*, 399.
[8] A. Srivastava, T. Yadav, S. Sharma, A. Nayak, A. A. Kumari, N. Mishra, *J. Biosci. Med.* **2015**, *4*, 69.
[9] K. Knop, R. Hoogenboom, D. Fischer, U. S. Schubert, *Angew. Chem. Int. Ed.* **2010**, *49*, 6288.

[10] T. G. Barclay, C. M. Day, N. Petrovsky, S. Garg, *Carbohydr. Polym.* **2019**, *221*, 94.
[11] Y. Sun, X. Jing, X. Ma, Y. Feng, H. Hu, *Int. J. Mol. Sci.* **2020**, *21*, 9159.
[12] J. Kurczewska, *Polymers* **2022**, *14*, 4189.
[13] J. Li, H. Xiang, Q. Zhang, X. Miao, *Pharmaceuticals* **2022**, *15*, 602.
[14] H. Hadji, K. Bouchemal, *Adv. Drug Deliv. Rev.* **2022**, *181*, 114101.
[15] M. A. Javaid, S. Jabeen, N. Arshad, K. M. Zia, M. T. Hussain, I. Ullah, S. Ahmad, M. Shoaib, *Sustain. Chem. Pharm.* **2023**, *33*, 101086.
[16] V. Sirisha, J. S. D'Souza, *Marine OMICS*, CRC Press, Florida **2016**.
[17] J. Zhang, P. Zhan, H. Tian, *Int. J. Biol. Macromol.* **2021**, *182*, 115.
[18] J. Pushpamalar, P. Meganathan, H. L. Tan, N. A. Dahlan, L.-T. Ooi, B. N. Neerooa, R. Z. Essa, K. Shameli, S.-Y. Teow, *Gels* **2021**, *7*, 153.
[19] W. Wei, J. Li, X. Qi, Y. Zhong, G. Zuo, X. Pan, T. Su, J. Zhang, W. Dong, *Carbohydr. Polym.* **2017**, *177*, 275.
[20] N. Yadav, A. P. Francis, V. V. Priya, S. Patil, S. Mustaq, S. S. Khan, K. J. Alzahrani, H. J. Banjer, S. K. Mohan, U. Mony, R. Rajagopalan, *Polymers* **2022**, *14*, 950.
[21] A. Basu, K. R. Kunduru, E. Abtew, A. J. Domb, *Bioconjug. Chem.* **2015**, *26*, 1396.
[22] S. Jiang, H. Chen, P. Shen, Y. Zhou, Q. Li, J. Zhang, Y. Chen, *Antioxid. Redox Signal.* **2023**, *40*, 168.
[23] A. Natarajan, G. J. Winner, *Int. J. Basic Clin. Pharmacol.* **2023**, *12*, 607.
[24] K. Abe, H. Kimura, *J. Neurosci.* **1996**, *16*, 1066.
[25] G. Cirino, C. Szabo, A. Papapetropoulos, *Physiol. Rev.* **2022**, *103*, 31.
[26] E. Magli, E. Perissutti, V. Santagada, G. Caliendo, A. Corvino, G. Esposito, G. Esposito, F. Fiorino, M. Migliaccio, A. Scognamiglio, B. Severino, R. Sparaco, F. Frecentese, *Biomolecules* **2021**, *11*, 1899.
[27] K. M. Dillon, H. A. Morrison, C. R. Powell, R. J. Carrazzone, V. M. Ringel-Scaia, E. W. Winckler, Council-Troche, R. M, I. C. Allen, J. B. Matson, *Angew. Chem. Int. Ed.* **2021**, *60*, 6061.
[28] A. G. Buret, T. Allain, J.-P. Motta, J. L. Wallace, *Antioxid. Redox Signal.* **2022**, *36*, 211.
[29] C. R. Powell, K. M. Dillon, J. B. Matson, *Biochem. Pharmacol.* **2018**, *149*, 110.
[30] C. M. Levinn, M. M. Cerda, M. D. Pluth, *Antioxid. Redox Signal.* **2020**, *32*, 96.
[31] S. Xu, M. Shieh, B. D. Paul, M. Xian, *Br. J. Pharmacol.* **2023**. https://doi.org/10.1111/bph.16211
[32] Z.-L. Song, L. Zhao, T. Ma, A. Osama, T. Shen, Y. He, J. Fang, *Med. Res. Rev.* **2022**, *42*, 1930.
[33] F. Rong, T. Wang, Q. Zhou, H. Peng, J. Yang, Q. Fan, P. Li, *Bioact. Mater.* **2023**, *19*, 198.
[34] S. Sarkar, R. Kumar, J. B. Matson, *Macromol. Biosci.* **2024**, *24*, 2300138.
[35] K. Kaur, R. J. Carrazzone, J. B. Matson, *Antioxid. Redox Signal.* **2019**, *32*, 79.
[36] H. Lu, Y. Chen, P. Hu, *Adv. Ther.* **2023**, *6*, 2200349.
[37] J. Hu, Y. Fang, X. Huang, R. Qiao, J. F. Quinn, T. P. Davis, *Adv. Drug Deliv. Rev.* **2021**, *179*, 114005.
[38] Z. Li, D. Li, L. Wang, C. Lu, P. Shan, X. Zou, Z. Li, *Polymer* **2019**, *168*, 16.
[39] N. V. Dao, F. Ercole, L. M. Kaminskas, T. P. Davis, E. K. Sloan, M. R. Whittaker, J. F. Quinn, *Biomacromolecules* **2020**, *21*, 5292.
[40] U. Hasegawa, A. J. van der Vlies, *Bioconjug. Chem.* **2014**, *25*, 1290.
[41] J. C. Foster, S. C. Radzinski, X. Zou, C. V. Finkielstein, J. B. Matson, *Mol. Pharm.* **2017**, *14*, 1300.
[42] C. M. Levinn, M. M. Cerda, M. D. Pluth, *Acc. Chem. Res.* **2019**, *52*, 2723.
[43] C. R. Powell, J. C. Foster, B. Okyere, M. H. Theus, J. B. Matson, *J. Am. Chem. Soc.* **2016**, *138*, 13477.
[44] A. K. Gilbert, M. D. Pluth, in *Hydrogen Sulfide: Chemical Biology Basics, Detection Methods, Therapeutic Applications, and Case Studies*, Wiley-VCH, Weinheim **2022**.
[45] M. D. Pluth, *Curr. Top. Med. Chem.* **2021**, *21*, 2882.
[46] K. Kaur, P. Enders, Y. Zhu, A. F. Bratton, C. R. Powell, K. Kashfi, J. B. Matson, *Chem. Commun.* **2021**, *57*, 5522.
[47] C. R. Powell, K. Kaur, K. M. Dillon, M. Zhou, M. Alaboalirat, J. B. Matson, *ACS Chem. Biol.* **2019**, *14*, 1129.
[48] C. R. Powell, J. C. Foster, S. N. Swilley, K. Kaur, S. J. Scannelli, D. Troya, J. B. Matson, *Polym. Chem.* **2019**, *10*, 2991.
[49] Q. Dong, B. Yang, J.-G. Han, M.-M. Zhang, W. Liu, X. Zhang, H.-L. Yu, Z.-G. Liu, S.-H. Zhang, T. Li, D. D. Wu, X. Y. Ji, S. F. Duan, *Cancer Lett.* **2019**, *455*, 60.
[50] A. J. van der Vlies, M. Ghasemi, B. M. Adair, J. H. Adair, E. D. Gomez, U. Hasegawa, *Adv. Healthc. Mater.* **2023**, *12*, 2201836.
[51] Y. Zhou, B. Yang, X. Ren, Z. Liu, Z. Deng, L. Chen, Y. Deng, L.-M. Zhang, L. Yang, *Biomaterials* **2012**, *33*, 4731.
[52] M. A. Javaid, S. Jabeen, N. Arshad, K. M. Zia, M. T. Hussain, I. A. Bhatti, A. Iqbal, S. Ahmad, I. Ullah, *Int. J. Biol. Macromol.* **2023**, *244*, 125224.
[53] R. Chang, M. Li, S. Ge, J. Yang, Q. Sun, L. Xiong, *Ind. Crop. Prod.* **2018**, *112*, 98.
[54] J. P. Mua, D. S. Jackson, *J. Agric. Food Chem.* **1997**, *45*, 3840.
[55] M. Wolfrom, J. Tyree, T. Galkowski, A. O'Neill, *J. Am. Chem. Soc.* **1951**, *73*, 4927.
[56] C. Li, Y. Hu, *Food Chem.* **2021**, *353*, 129449.
[57] P. Salemis, M. Rinaudo, *Polym. Bull.* **1984**, *12*, 283.
[58] D. S. Kazybayeva, G. S. Irmukhametova, V. V. Khutoryanskiy, *Polym. Sci., Ser. B* **2022**, *64*, 1.
[59] E. Abedi, S. Savadkoohi, S. Banasaz, *Food Chem.* **2023**, *410*, 135261.
[60] D. Trimnell, B. Shasha, W. Doane, C. Russell, *J. Appl. Polym. Sci.* **1973**, *17*, 1607.
[61] Y. Li, Y. Tan, K. Xu, C. Lu, P. Wang, *Polym. Degrad. Stab.* **2017**, *137*, 75.
[62] K. Chauhan, V. Priya, P. Singh, G. S. Chauhan, S. Kumari, R. K. Singhal, *RSC Adv.* **2015**, *5*, 51762.
[63] D. Trimnell, E. I. Stout, W. M. Doane, C. R. Russell, *J. Appl. Polym. Sci.* **1977**, *21*, 655.
[64] A. C. Ribeiro, Â. Rocha, R. M. Soares, L. P. Fonseca, N. P. da Silveira, *Carbohydr. Polym.* **2017**, *157*, 267.
[65] I. Rashid, M. H. A. Omari, S. A. Leharne, B. Z. Chowdhry, A. Badwan, *Starch-Stärke* **2012**, *64*, 713.
[66] J. C. Foster, C. R. Powell, S. C. Radzinski, J. B. Matson, *Org. Lett.* **2014**, *16*, 1558.

[67] M. M. Cerda, J. L. Mancuso, E. J. Mullen, C. H. Hendon, M. D. Pluth, *Chem. – A Eur. J.* **2020**, *26*, 5374.
[68] X. Ni, X. Li, T.-L. Shen, W.-J. Qian, M. Xian, *J. Am. Chem. Soc.* **2021**, *143*, 13325.
[69] Q. Hu, S. I. Suarez, R. A. Hankins, J. C. Lukesh III, *Angew. Chem. Int. Ed.* **2022**, *61*, e202210754.
[70] H. M. Smith, M. D. Pluth, *JACS Au* **2023**, *3*, 2677.
[71] T. H. Baryakova, B. H. Pogostin, R. Langer, K. J. McHugh, *Nat. Rev. Drug Discov.* **2023**, *22*, 387.
[72] P. H. Redfern, B. Lemmer, *Physiology and pharmacology of biological rhythms*, Springer Science & Business Media, New York **2013**.

SUPPORTING INFORMATION

Additional supporting information can be found online in the Supporting Information section at the end of this article.

How to cite this article: A. F. Chinn, N. R. Williams, K. M. Miller, J. B. Matson, *J. Polym. Sci.* **2024**, *62*(18), 4155. https://doi.org/10.1002/pol.20240262